

A Decanuclear Iron(III) Single Molecule Magnet: Use of Monte Carlo Methodology To Model the Magnetic Properties

Cristiano Benelli,[†] Joan Cano,[‡] Yves Journaux,^{*,‡} Roberta Sessoli,[†] Gregory A. Solan,[§] and Richard E. P. Winpenny^{*,||}

Department of Chemistry, University of Florence, Via Maragliano 77, 50144 Florence, Italy, Laboratoire de Chimie Inorganique, UMR CNRS 8613 Université Paris-Sud, 91405 Orsay, France, Department of Chemistry, University of Leicester, University Road, Leicester LE1 7RH, U.K., and Department of Chemistry, University of Manchester, Oxford Road, Manchester M13 9PL, U.K.

Received July 26, 2000

The observation that metal clusters can show slow relaxation of magnetization¹ is intriguing both from a technological point of view and because of the potential impact on fundamental science. The most well-known system is based on the {Mn₁₂} family,^{1,2} but other examples are known.^{3–7} These discoveries have stimulated efforts to make more single-molecule magnets (SMMs), and to reexamine previously reported high-spin cages to check whether they also have an energy barrier to reorientation of magnetization.

A putative candidate is an {Fe₁₀^{III}} cage of formula [Fe₁₀Na₂(O)₆(OH)₄(O₂CPh)₁₀(chp)₆(H₂O)₂(Me₂CO)₂] **1** (chp = 6-chloro-2-pyridonato) with a *S* = 11 ground state.⁸ We have been unable to model the susceptibility behavior using matrix-diagonalization techniques due to the large size of the cage and its low symmetry (*C*_{2h}). Similar problems have been found for other high-nuclearity cages in which *S* = 5/2 centers interact.^{9,10} Here we report the first use of Monte Carlo methods to model susceptibility behavior within a discrete cluster, which confirms the high-spin ground state. Moreover, ac susceptibility measurements show that **1** is a new SMM.

For **1**, the room temperature value of the product $\chi_M T$ is 34.35 cm³ K mol⁻¹, which is lower than that expected for magnetically isolated Fe(III) ions (Figure 1). However, the value of $\chi_M T$ increases steadily down to 40 K, where a maximum is reached at a $\chi_M T$ value of 64.7 cm³ K mol⁻¹. Below 40 K, $\chi_M T$ decreases smoothly, reaching a value of 63.9 cm³ K mol⁻¹ at 20 K that corresponds to the theoretical value expected for a *S* = 11 ground

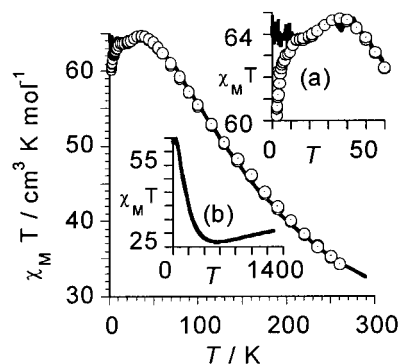


Figure 1. Experimental (open circles) and MC simulation (line) plots of $\chi_M T$ against *T* for **1**. Inset a: magnification of the maximum at 40 K. Inset b: MC simulation for the 1400–2 K temperature range.

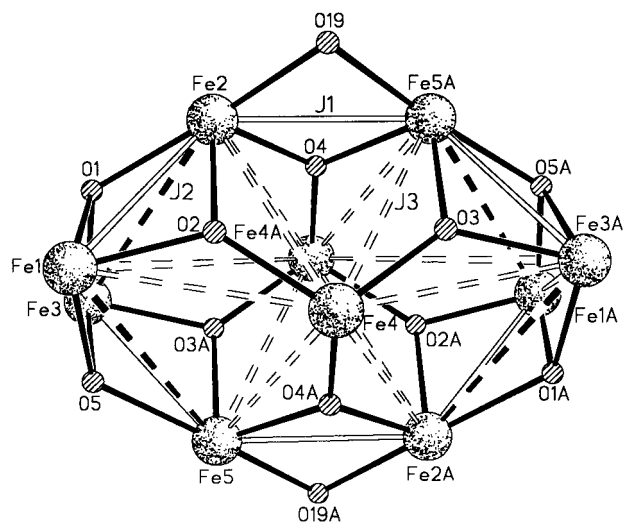


Figure 2. The core of **1** showing the atom numbering and the exchange coupling scheme. Fe–O bonds shown as full lines; *J*₁ shown as open lines; *J*₂ shown as dashed full lines; *J*₃ shown as dashed open lines.

state (Figure 2 inset a). Below this temperature an abrupt fall in $\chi_M T$ is observed, which could be due to zero field splitting (ZFS) and/or antiferromagnetic intermolecular interactions.

The high spin of the cage and the plateau in the plot of $\chi_M T$ against *T* led us to examine the relaxation behavior of **1**. Below 1 K a signal is seen in the out-of-phase susceptibility, and the temperature at which this signal is a maximum is frequency dependent, which is a signature for a SMM. From the frequency dependence we can use an Arrhenius plot to derive an energy barrier for reorientation of the magnetization for **1** of 5.3 K.

In the temperature range 300–20 K, the Monte Carlo simulations have been performed using the Metropolis algorithm which generates a sampling of states following the Boltzmann distribu-

[†] University of Florence.

[‡] UMR CNRS 8613 Université Paris-Sud.

[§] University of Leicester.

^{||} University of Manchester.

- (1) (a) Sessoli, R.; Tsai, H.-L.; Schake, A. R.; Wang, S.; Vincent, J. B.; Folting, K.; Gatteschi, D.; Christou, G.; Hendrickson, D. N. *J. Am. Chem. Soc.* **1993**, *115*, 1804–1816. (b) Sessoli, R.; Gatteschi, D.; Caneschi, A.; Novak, M. A. *Nature* **1993**, *365*, 141–142.
- (2) Sun, Z. M.; Ruiz, D.; Rumberger, E.; Incarvito, C. D.; Folting, K.; Rheingold, A. L.; Christou, G.; Hendrickson, D. N. *Inorg. Chem.* **1998**, *37*, 4758–4759.
- (3) Sangregorio, C.; Ohm, T.; Paulsen, C.; Sessoli, R.; Gatteschi, D. *Phys. Rev. Lett.* **1997**, *78*, 4645–4648.
- (4) Sun, Z.; Grant, C. M.; Castro, S. L.; Hendrickson, D. N.; Christou, G. *Chem. Commun.* **1998**, 721–722.
- (5) (a) Wemple, M. W.; Adams, D. M.; Hagen, K. S.; Folting, K.; Hendrickson, D. N.; Christou, G. *J. Chem. Soc., Chem. Commun.* **1995**, 1591–1593. (b) Brechin, E. K.; Yoo, J.; Nakano, M.; Huffman, J. C.; Hendrickson, D. N.; Christou, G. *Chem. Commun.* **1999**, 783–784.
- (6) Barra, A. L.; Caneschi, A.; Gatteschi, D.; Goldberg, D. P.; Sessoli, R. *J. Solid State Chem.* **1999**, *145*, 484–487.
- (7) Barra, A. L.; Caneschi, A.; Cornia, A.; deBiani, F. F.; Gatteschi, D.; Sangregorio, C.; Sessoli, R.; Sorace, L. *J. Am. Chem. Soc.* **1999**, *121*, 5302–5310.
- (8) Benelli, C.; Parsons, S.; Solan, G. A.; Winpenny, R. E. P. *Angew. Chem., Int. Ed. Engl.* **1996**, *35*, 1825–1828.
- (9) Powell, A. K.; Heath, S. L.; Gatteschi, D.; Pardi, L.; Sessoli, R.; Spina, G.; Del Giallo, F.; Pieralli, F. *J. Am. Chem. Soc.* **1995**, *117*, 2491–2502.
- (10) Taft, K. L.; Delfs, C. D.; Papaefthymiou, G. C.; Foner, S.; Gatteschi, D.; Lippard, S. J. *J. Am. Chem. Soc.* **1994**, *116*, 823–832.

tion.^{11,12} The interaction energy between magnetic centers, without considering ZFS effects, is calculated using classical spins scaled according to the factor $S_j = (S_j(S_j + 1))^{1/2}$. The reliability of this approach for discrete systems has been previously checked on small clusters where the exact solution is available from conventional modeling approaches.¹³ The reproducibility of the simulation has been tested using different starting conditions.

The five chemically distinct Fe \cdots Fe exchange interaction pathways found in **1** can be grouped in two distinct structural types, a single μ -OX and a double-bridge (μ -OX)₂, where OX stands for OH (hydroxo), OR (chp), and OFe (μ_3 -O²⁻, oxo). The exchange parameter J_1 was used to account for the three interactions where the superexchange path is bridged by two atoms (Figure 2). These are as follows: the exchanges Fe1 \cdots Fe2, Fe3 \cdots Fe5 and their symmetry equivalents (se), which are bridged by one μ_3 -oxide (O2 and O3A respectively) with Fe–O–Fe angles of $100.7^\circ \pm 0.1^\circ$ and one μ_3 -hydroxide (O1 and O5 respectively) with Fe–O–Fe angles of 91.4° and 90.9° ; the exchanges Fe2 \cdots Fe5A and Fe2A \cdots Fe5, which are bridged by one μ_3 -oxide (O4 or O4A, Fe–O–Fe angle 100.6°) and a μ_2 -oxygen from a chp ligand (Fe–O–Fe angle 95.7°); and the exchanges Fe1 \cdots Fe3 and Fe1A \cdots Fe3A, which are bridged by two μ_3 -hydroxides (O1, O5 and se) with Fe–O–Fe angles of 97.4° and 99.7° .

The exchange parameter J_2 accounts for coupling bridged exclusively by a single hydroxide (Figure 2). This occurs four times in the model, between Fe1 \cdots Fe5, Fe2 \cdots Fe3, and the se interactions. The Fe–O–Fe angles are between 128.7° and 129.9° . J_3 accounts for exchange mediated by single oxide bridges and occurs 12 times in the model, between Fe4 and six iron centers (Fe1, Fe2, Fe5A, Fe3A, Fe2A, and Fe5) and similarly between Fe4A and the six irons (Fe1A, Fe2A, Fe5, Fe3, Fe2A, Fe5A). The angles at these oxide bridges are consistent, ranging from 126.8° to 130.2° . The Hamiltonian used is given in eq 1.

$$\begin{aligned}
 H = & -J_1[S_1 \cdot S_2 + S_2 \cdot S_{5A} + S_{5A} \cdot S_{3A} + S_{3A} \cdot S_{1A} + \\
 & S_{1A} \cdot S_{2A} + S_{2A} \cdot S_5 + S_5 \cdot S_3 + S_3 \cdot S_1] \\
 & - J_2[S_1 \cdot S_5 + S_2 \cdot S_3 + S_{1A} \cdot S_{5A} + S_{2A} \cdot S_{3A}] \\
 & - J_3[S_4\{S_1 + S_2 + S_{3A} + S_{2A} + S_{5A} + S_5\} + \\
 & S_{4A}\{S_{1A} + S_2 + S_3 + S_{2A} + S_{5A} + S_5\}] \quad (1)
 \end{aligned}$$

Preliminary simulations showed that the experimental curve can be reproduced only for $J_1 \gg J_2, J_3$. Several simulations with different α_2 and α_3 values have been performed, α_i being the ratio J_i/J_1 .¹³ The existence of competitive interactions within the cluster leads to a strong correlation between the J_2 and J_3 parameters. However, in the 40–20 K range only one set of J_2 and J_3 parameters were able to reproduce the smooth decrease of $\chi_M T$ (see inset a in Figure 2). The best fit parameters are $J_1 = -44 \text{ cm}^{-1}$, $J_2 = -13 \text{ cm}^{-1}$, and $J_3 = -10 \text{ cm}^{-1}$. Despite all the interactions being antiferromagnetic, these parameters perfectly reproduce the increase of $\chi_M T$ down to 40 K. The presence of

competitive antiferromagnetic interactions inside the cluster leads to a theoretical minimum for $\chi_M T$ around 560 K (see inset b of Figure 2).

The strongest exchange in **1** is mediated by two bridging groups (J_1). With an average bridging angle of 96.4° , crossed interactions¹⁴ are expected to be very efficient for oxo, hydroxo, and pyridonato bridges, i.e., a good overlap between the magnetic orbitals on both sides of the bridge occurs. The overlap between the magnetic orbitals varies slightly with the angle,^{14–16} and consequently in **1**, all bridges lead to a similar overlap between the magnetic orbitals. The J_1 value is smaller than that observed in bis(μ -oxo)diiron(III) complexes (-54 cm^{-1}), despite the observed acute Fe–O–Fe angle. This may be related to the unusually large Fe–O(oxo) bond length in **1** ($1.900\text{--}1.951 \text{ \AA}$ vs $1.73\text{--}1.83 \text{ \AA}$).¹⁷ The value is larger than that observed in bis(μ -alkoxo)diiron(III) complexes (J varies from -15 to -25 cm^{-1} depending on the Fe–O–Fe angle).¹⁸

A decrease of the oxygen-pathway electronic density due to the presence of the X group would lead to a larger Fe–O bond length and, concomitantly, a weaker magnetic exchange interaction between iron(III) ions, in agreement with the correlation between the J values and the Fe–O distances found by Lippard.¹⁴ For Fe(III) complexes containing the dinuclear [$\text{Fe}_2(\mu\text{-AcO})_2(\text{Y})$] core, where Y = μ -O, μ -OH, or μ -OFe (equivalent to μ_3 -O), the Fe–O bond lengths are shorter for μ -oxo (1.78 \AA)¹⁹ than for μ -hydroxo (1.97 \AA)¹⁹ or μ_3 -oxo (1.90 \AA);^{20,21} and the magnetic interactions are stronger for μ -oxo (-80 to -100 cm^{-1})¹⁹ than for μ -hydroxo (-17 cm^{-1})¹⁹ or μ_3 -oxo (from -8 to -10 cm^{-1}).^{20,21} Thus, for a μ_3 -oxo bridge (noted above as μ -OFe) the third iron atom plays a role similar to that of the hydrogen atom in the μ -OH bridge. For **1**, as in these previous examples, the interaction mediated by the single μ_3 -oxo bridge ($J_3 = -10 \text{ cm}^{-1}$) is of the same order of magnitude as that through the monohydroxo bridge μ_3 -OH ($J_2 = -13 \text{ cm}^{-1}$). It is not obvious why the value for single μ_3 -oxo bridges should fall in this range.

In summary, our results open up the possibility of using Monte Carlo methodology to model the magnetic behavior of other high-nuclearity iron clusters with low-symmetry topologies.²² **1** is the third iron-containing SMM reported. The first example,³ an $\{\text{Fe}_8\}$ cage, has a $S = 10$ ground state and a reorientation barrier of 28 K. The height of this barrier is given by DS^2 (where D is the axial zero-field splitting parameter and S is the spin of the ground state), and therefore the higher barrier for $\{\text{Fe}_8\}$ must be related to a larger D value.

Acknowledgment. This work was supported by the EPSRC (U.K.) and by The Royal Society of Edinburgh, NATO and by the EU under the TMR Programme “Molecules as Nanomagnets” (HPRN-CT-1999-00012) and by a Marie Curie grant (No. EERBFMBICT972211).

IC000840E

- (11) Metropolis, N.; Rosenbluth, A. W.; Rosenbluth, M. N.; Teller, A. H.; Teller, E. *J. Chem. Phys.* **1953**, *21*, 1087.
- (12) The size of the sample is the whole decanuclear iron core of the complex. For all the simulations, 5×10^5 Monte Carlo steps were performed per site (MCS) and the first 5×10^4 were discarded as the initial transient stage. To avoid the freezing of the spin configuration, a low cooling rate was used according to the equation $T_{n+1} = 0.95T_n$, where T stands for temperature. For more details see: Cano Boquera, J.; Journaux, Y. *Mol. Cryst. Liq. Cryst.* **1999**, *335*, 685. Goher, M. A. S.; Cano, J. Y.; Journaux, M. A. M.; Abu-Youssef, F. A.; Mautner, A.; Escuer, R.; Vicente, *Chem. Eur. J.* **2000**, *6*, 778–784.
- (13) Cano Boquera, J.; Boullant, E.; Journaux, Y. Manuscript in preparation.

- (14) Hotzelmann, R.; Wieghardt, K.; Flörke, U.; Haupt, H.-J.; Weatherburn, D. C.; Bonvoisin, J.; Blondin, G.; Girerd, J.-J. *J. Am. Chem. Soc.* **1992**, *114*, 1681–1696.
- (15) Gorun, S. M.; Lippard, S. J. *Inorg. Chem.* **1991**, *30*, 1625–1630.
- (16) Weihe, H.; Güdel, H. U. *J. Am. Chem. Soc.* **1998**, *120*, 2870–2879.
- (17) Zang, Y.; Dong, Y.; Que, L. *J. Am. Chem. Soc.* **1995**, *117*, 1169–1170.
- (18) Le Gall, F.; Fabrizi de Biani, F.; Caneschi, A.; Cinelli, P.; Cornia, A.; Fabretti, A. C.; Gatteschi, D. *Inorg. Chim. Acta* **1997**, *262*, 123–132.
- (19) Kurtz, D. M. *Chem. Rev.* **1990**, *90*, 585–606.
- (20) Reynolds, R. A., III; Dunham, W. R.; Coucouvanis, D. *Inorg. Chem.* **1998**, *37*, 122–1241.
- (21) Wemple, M. W.; Coggin, D. A. K.; Vincent, J. B.; McCusker, J. K.; Streib, W. E.; Huffman, J. C.; Hendrickson, D. N.; Christou, G. *Dalton Trans.* **1998**, 719–725.
- (22) Parsons, S.; Solan, G. A.; Winpenny, R. E. P. *J. Chem. Soc., Chem. Commun.* **1995**, 1987.